Functional Role of a Conserved Aspartate in the External Mouth of Voltage-Gated Potassium Channels

Glenn E. Kirsch,*‡ Juan M. Pascual,* and Char-Chang Shieh*
Departments of Molecular Physiology and Biophysics* and Anesthesiology,‡ Baylor College of Medicine, Houston Texas 77030 USA

ABSTRACT Mutation of the glycines in a conserved Gly-Tyr-Gly-Asp sequence in the P-region of voltage-gated K channels has identified determinants of Na/K selectivity. But the function of the negatively charged Asp is not known because mutations at this position are not tolerated, owing to the fourfold replication of mutations in a tetrameric channel. We have successfully mutated $Asp^{378} \rightarrow Thr$ in a tandem dimer $K_v2.1$ construct to yield a twofold neutralization of charge at this site. When expressed in *Xenopus* oocytes, the mutated channels showed markedly altered ion conduction and blockade. Potassium conduction in the inward direction was selectively reduced, so that the instantaneous current-voltage relationship obtained in isotonic KCl became strongly outwardly rectifying. The relative permeability to Na^+, P_{Na}/P_K, increased from 0.02 to 0.10 without changing the ion selectivity sequence $K > Rb \gg Cs \gg Na$. The IC_{50} for block by external tetraethylammonium (TEA) increased more than 100-fold without affecting block by internal TEA. We conclude that Asp^{378} is an essential part of a potassium ion binding site associated with the Na/K selectivity filter at the external mouth of the pore.

INTRODUCTION

The notion that cation-selective channels contain negatively charged groups has been supported by the identification of acidic amino acid residues in the ion-conducting pathways (pores) of a variety of cloned cation channels, including ligand-gated channels associated with cyclic nucleotide (Root and MacKinnon, 1993), acetylcholine (Imoto et al., 1988), as well as voltage-gated Na (Noda et al., 1989) and Ca channels (Tang et al., 1993; Yang et al., 1993). In voltage-gated K (K_v) channels several negatively charged residues in the external mouth have been shown to be binding determinants for cationic blockers such as charybdotoxin (CTX; MacKinnon and Miller, 1989a) and tetraethylammonium (TEA; MacKinnon and Yellen, 1990); however, these amino acids are not well conserved among K_v channels and therefore may not be important for fundamental pore properties.

In K_v channels the external mouth and a substantial part of the pore have been localized to a 21 peptide segment (P-region, Fig. 1) of the S5–S6 linker, and analogous segments have been identified in other K-selective channel clones, such as the large conductance Ca-dependent (K_{Ca}; Butler et al., 1993) channel. Within the P-region of K_v channels, two glycines in a conserved Gly-Tyr-Gly-Asp motif have been identified as important determinants of cation selectivity (Heginbotham et al., 1994), but the functional role of the Asp is unknown because neutralization of this residue by mutation prevents expression of K currents (Goldstein et al., 1994). The problem of nonexpression of pore mutants may arise in part because each mutation is replicated fourfold in the tetrameric channel. To overcome this problem we have mutated $Asp^{378} \rightarrow Thr$ (D378T) of the GYGD sequence, in a tandem dimer $K_v2.1$ construct in which the mutation appears in only one subunit, thus reducing the mutation dosage by twofold. When expressed in *Xenopus* oocytes, the mutated channels showed markedly altered conduction, selectivity, and blockade. These results show that a conserved Asp^{378} (corresponding to Asp^{447} in *Shaker*) is part of a potassium ion binding site associated with the Na/K selectivity filter in the external mouth of the pore.

MATERIALS AND METHODS

Rat brain K channel tandem dimer cDNA constructs

As shown in Fig. 2, a dimer cDNA was constructed that linked two $K_v2.1$ subunits together covalently. Repeat 1 consisted of a full $K_v2.1$ amino terminus including the initiation Met in the first repeat, complete membrane spanning core, and C-terminus with 351 amino acid deletion. An artificial linker between repeats 1 and 2 encoded six amino acids. Repeat 2 consisted of an N-terminus with a 121 amino acid deletion, the complete membrane spanning core, and a C-terminus with 290 amino acid deletion. The deletions were introduced to reduce the size of the construct to facilitate DNA work and to remove in-frame methionines that precede the core region of repeat 2, to prevent translation of partially degraded cRNA. Both repeats contained the minimal sequence required for functional $K_v2.1$ expression, extending 33 amino acids upstream from S1 and 30 residues downstream from S6 (VanDongen et al., 1990). The ΔN121 deletion left intact only one Met^{139} with very low translation initiation in the second dimer repeat (VanDongen et al., 1990).

$K_v2.1$ dimers were constructed in several steps. 1) A ΔC290 $K_v2.1$ deletion construct (downstream repeat) was digested at the *Xho*I (plasmid polylinker) and *Bsp*106I sites to generate a vector suitable for ligation at the 5′ end with another repeat. 2) A second $K_v2.1$ clone (upstream repeat) was digested with *Xho*I and *Bam*HI (1541). 3) The *Bam*HI end of the insert was made compatible with the *Bsp*106I end of the vector by ligation of an adaptor oligonucleotide pair that encoded both *Bam*HI and *Bsp*106I ends, and a central unique *Nsi*I site. The adaptor serves as an artificial linker that adds six new amino acids (SQMHQF) in frame between each repeat. The vector in which the construct was made also contains a portion of the $K_v2.1$ 3′-untranslated region, including the poly-A tail to facilitate expression of the dimer construct in oocytes.

Received for publication 28 November 1994 and in final form 23 February 1995.

Address reprint requests to Dr. G.E. Kirsch at his present address, Rammelkamp Center for Education and Research, MetroHealth Medical Center, 2500 MetroHealth Drive, Cleveland, OH 44109–1998. Tel.: 216-459-5955; Fax: 216-778-8282.

0006-3495/95/05/1804/10 $2.00

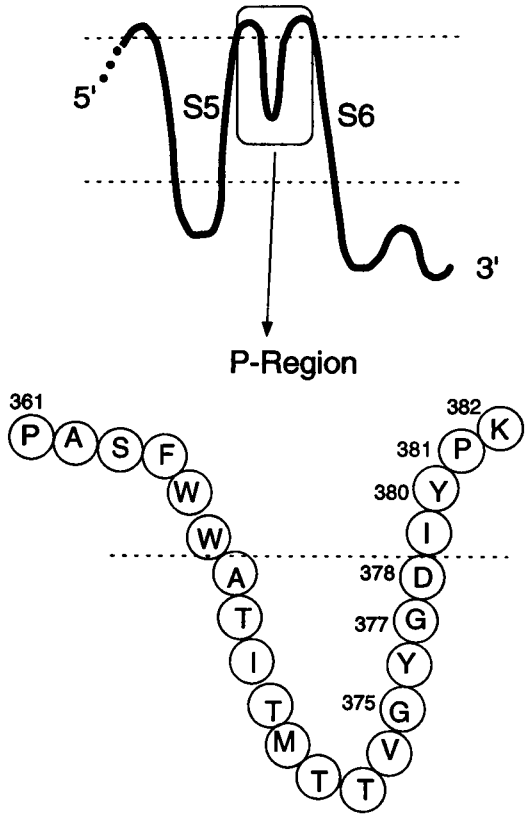

FIGURE 1 $K_v2.1$ P-region. The upper diagram shows the membrane-folding pattern of the C-terminal half of K_v channels, including S4–S6. The pore-forming (P) region is designated as a 21 residue segment (*lower diagram*) of the S5–S6 linker bounded by two prolines at positions 361 ($K_v2.1$ numbering equivalent to *Shaker* Pro^{430}) and 381 (*Shaker* Pro^{450}). The mutation described in this paper is Asp^{378} (*Shaker* Asp^{447}) → Thr.

We used two functional assays to test whether the tandem dimers expressed channels with appropriate subunit stoichiometry. First, we took advantage of the distinct single channel conductances specified by the WT monomer and a chimeric construct in which the P-region of $K_v2.1$ was replaced by that of $K_v3.1$ (Hartmann et al., 1991). The following dimer constructs were made and expressed in *Xenopus* oocytes: homodimers of WT-WT and CHM-CHM, and heterodimers of WT-CHM and CHM-WT.

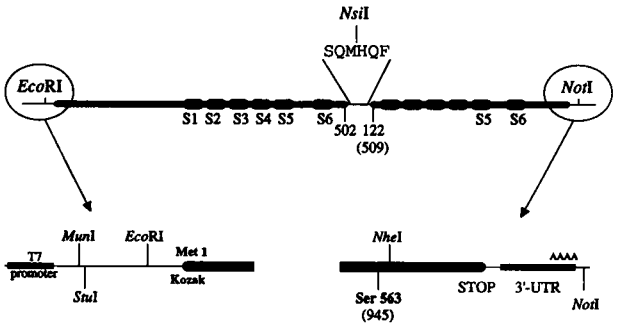

FIGURE 2 Linear scheme for a tandem dimer $K_v2.1$ clone consisting of two truncated $K_v2.1$ clones linked by an adaptor segment (SQMHQF). The lower, expanded diagrams show the promoter and Kozak initiation sequence encoded at the N-terminus, and the stop codon and poly-A tail (in the 3' untranslated region) encoded at the C-terminus. Numbers indicate original $K_v2.1$ amino acid positions. Numbers in parentheses refer to dimer positions.

As expected, homodimers expressed channels with uniform conductances of 8.8 ± 0.5 pS (n = 4) and 25.9 ± 1.8 pS (n = 7), respectively, which are nearly identical to the values obtained previously in WT and CHM. Significantly, heterodimers of WT-CHM and CHM-WT each expressed a homogenous population of channels with uniform conductances of 19.5 ± 1.1 pS (n = 5) and 19.2 ± 0.8 pS (n = 6). In the heterodimer test, the lack of subpopulations expressing WT or CHM phenotypes suggests that the subunit stoichiometry was tightly specified by the dimer construction. A second assay was to construct a mutant dimer, Y380C-WT, in which the sensitivity to external TEA should be markedly reduced compared with WT-WT. The mutant dimer, Y380C monomer, and WT dimer each expressed a homogenous population of channels with sensitivity to TEA that could be fit accurately by 1:1 binding isotherms; the IC_{50} values were 14.2 ± 0.04 mM (n = 5), 34.5 ± 0.02 mM (n = 9), and 5.7 ± 0.01 mM (n = 4) in, respectively, mutant dimer, mutant monomer, and WT dimer. Thus, in the heterodimer the lack of a subpopulation of channels with WT TEA sensitivity also indicates a tightly controlled stoichiometry.

Mutations

D378T and K382C mutations were introduced by polymerase chain reaction (PCR) into a ΔC351 $K_v2.1$ cDNA construct. This monomeric construct contained four unique restriction sites (both natural and engineered) that provide convenient points for vector preparation. PCR reactions were performed between the mutant primer containing the upstream site and a reverse orientation primer that contains the downstream site. The PCR products were digested with the appropriate restriction enzymes to yield mutant inserts. The insert was ligated back into a $K_v2.1$ cDNA fragment that has been digested with the appropriate restriction enzymes. The mutation was confirmed by sequence analysis of the entire ligated fragment.

RNA transcription and oocyte injection

DNA constructs were linearized at the 3' ends by digestion with *NotI* for runoff transcription. In vitro transcription with T7 RNA polymerase was performed using the mMessage mMachine kit (Ambion, Austin TX). The amount of cRNA synthesized (20–100 μg) was quantified by the incorporation of trace amounts of [^{32}P]UTP in the synthesis mixture. The final cRNA product was resuspended in 0.1 M KCl at a final concentration of 250 ng/μl and stored at −80°C. The integrity of the final product and the absence of degraded RNA was determined by denaturing agarose gel stained with ethidium bromide. The cRNA was diluted to the desired concentrations (generally 1–10 pg/nl) immediately before oocyte injection. Stage V and VI *Xenopus* oocytes were defolliculated by collagenase treatment (2 mg/ml for 1.5 h) in a Ca-free buffer solution (in mM): NaCl 82.5, KCl 2.5, $MgCl_2$ 1, HEPES 5 (+100 μg/ml gentamicin), pH 7.6. The defolliculated oocytes were injected with 46 nl of cRNA solution (in 0.1 M KCl) and incubated at 19°C in culture medium (in mM): NaCl 100, KCl 2, $CaCl_2$ 1.8, $MgCl_2$ 1, HEPES 5, Pyruvic acid 2.5 (+100 μg/ml gentamicin), pH 7.6. Electrophysiological measurements were made 2–6 days after cRNA injection.

Electrophysiology and data analysis

Whole cell currents were recorded in oocytes using a two-intracellular microelectrode voltage clamp as described previously (Drewe et al., 1994). Bevelled microelectrode tips were filled with a solution of 3 M KCl + 1% agar and then backfilled with 3 M KCl (Schreibmayer et al., 1994). This method gave sharp-tipped microelectrodes with low electrical resistance (0.2–0.5 MΩ) required for optimal clamp performance. With this method the input resistance of oocytes impaled with two microelectrodes was in the range 0.4–0.5 MΩ. Oocytes with input resistance below this level were considered to be damaged and were discarded. Linear leakage and capacitative transient currents were subtracted online using a P/4 subtraction routine. Tail current amplitudes and reversal potentials were determined from the value extrapolated to the start of the test pulse by fitting a monoexponential function to the decay phase.

Cell-attached patch recording was performed after manual removal of the vitelline envelope. Isotonic KCl bathing solution was used to zero the resting potential; the absence of resting membrane potential was verified by rupturing the membrane patch at the end of each experiment to allow direct intracellular potential measurement. Holding and test potentials applied to the membrane patch during the experiment are reported as conventional intracellular potentials. Channels were activated with rectangular test pulses from negative holding potentials. Data were low pass filtered at 5 kHz (−3 dB, four-pole Bessel filter), then digitized at 20–100 kHz. Linear leakage and capacitative currents were subtracted digitally using the smoothed average of 5–10 null traces in which no channel openings could be detected. Open and closed transitions were detected using a half-amplitude threshold criterion. Single channel current-voltage relationships obtained from amplitude histograms were tabulated from idealized currents at test pulse potentials −50 to +20 mV.

The analysis of membrane current fluctuations in macropatch experiments to obtain an estimate of single channel conductance was performed according to the method of Sigworth (1980). Briefly, cell-attached macropatches were repetitively stimulated at 1 Hz using test pulses to 0 mV from a holding potential of −100 mV, and a sample of 16–32 consecutive traces was analyzed in each patch. Leakage and capacitative currents were subtracted by the null trace method described above. To minimize the effects of drift during the recording period, the variance at each sample point in a given trace was calculated from the local mean obtained by pairwise averaging of the analyzed trace with the next trace (Heinemann et al., 1992). A sample of the baseline variance, consisting primarily of thermal noise, was measured during hyperpolarizing steps. Total variance was corrected by subtracting the average baseline variance. The corrected, ensemble average variance at each time point was plotted against the ensemble average current, and the data were fit by adjusting the two free parameters in the function (Sigworth, 1980):

$$\sigma^2 = i * I - (I^2/N), \quad (1)$$

where I and σ^2 are the mean and variance of the membrane current, N is the total number of active channels in the patch, and i is the single channel current.

Data were expressed as means ± SEM where appropriate. A two-tailed Student's t-test was used to evaluate the significance of the difference between means ($p < 0.05$).

Solutions and drugs

A modified Ringer's solution for whole cell recording consisted of (in mM): 120 NaCl, 1 $CaCl_2$, 2 $MgCl_2$, 10 HEPES, pH 7.2 (with Tris-OH). This basic solution was adapted to the needs of different experiments, as noted in the text by replacing 120 mM NaCl with other mixtures of salts. Thus, in selectivity experiments NaCl was replaced by 120 mM KCl, RbCl, or CsCl. The control solution for ionic strength experiments consisted of (in mM): 20 KCl, 100 LiCl, 5 HEPES, pH 7.2 (with Tris-OH). This solution is nominally Ca-free to minimize divalent ion screening of surface charge. LiCl was used as an impermeant substitute, which prevents the increase in leakage conductance often observed in Na-containing, Ca-free solutions (L. Parent, personal communication). Ionic strength was reduced by replacing 100 mM LiCl with 200 mM sucrose.

Depolarizing isotonic KCl bath solution for patch recording consisted of (in mM): 100 KCl, 10 EGTA, 10 HEPES, pH 7.3. Pipette solution consisted of (in mM): 120 KCl, 1 $CaCl_2$, 2 $MgCl_2$, 10 HEPES, pH 7.2. Bathing solution flowed continuously at a rate of 3 ml/min. All electrophysiological measurements were made at room temperature (21–23°C).

RESULTS

Mutation of several nonconserved acidic residues in the external mouth of the *Shaker* pore has shown that these residues influence CTX (MacKinnon and Miller, 1989a; Goldstein et al., 1994) and TEA block (MacKinnon and Yellen, 1990), but a conserved residue, Asp^{447}, could not be tested because mutation did not give functional channels (Goldstein et al., 1994). We found that in the *Shab*-related, $K_v2.1$, mutation of the corresponding aspartate, Asp^{378}, to Thr (D378T, a mutation that conserved side chain volume, but neutralized charge) also failed to express currents, even when the cRNA was injected at a high concentration (20 pg/nl, Fig. 3 *A*). The possibility that the mutation produced nonselective, voltage-insensitive "leakage current" channels was excluded by measuring leakage current at a holding potential of −80 mV. In uninjected oocytes or oocytes injected with either of the WT channels that are closed at −80 mV, we obtained leakage currents in the range 0.15–0.2 μA. We observed no significant increase in leakage current in oocytes injected with D378T monomer cRNA.

By contrast, when the D378T mutation was performed only in the first repeat of a tandem dimer $K_v2.1$ construct, injection of cRNA concentration at reduced concentration (2 pg/nl) produced robust voltage-gated currents (Fig. 3 *B*) that displayed a waveform similar to that of unmutated channels expressed by wild-type dimer constructs (WT, Fig. 3 *C*, 1 pg/nl). From records such as these we obtained Boltzmann fits of the voltage dependence of activation, with midpoint potentials that were not significantly different between WT ($V_{0.5}$ = 8.5 ± 3.4 mV, n = 7) and D378T ($V_{0.5}$ = 7.7 ± 3.1

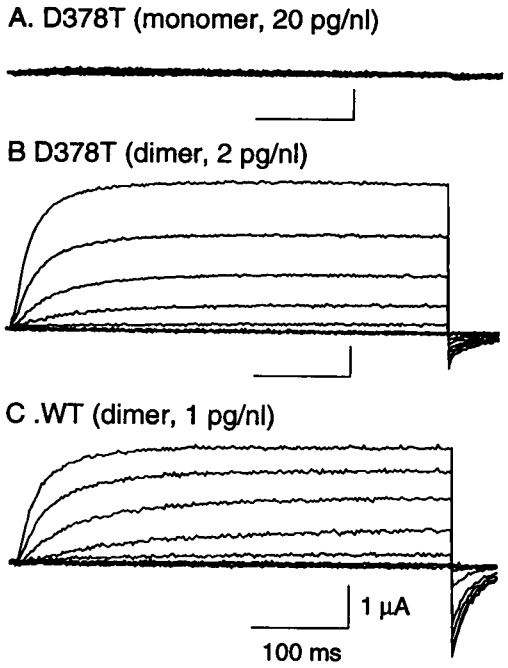

FIGURE 3 Expression of $K_v2.1$ tandem dimer constructs in *Xenopus* oocytes. Each current-voltage (I-V) family of traces was obtained from different oocytes 4 days after injection with cRNA encoding D378T monomer construct (*A*, 20 pg/nl), D378T dimer construct (*B*, 2 pg/nl), or WT dimer construct (*C*, 1 pg/nl). Superimposed current records were evoked by a series of test pulses (450 ms duration) ranging from −40 to +40 mV in 10 mV increments from a holding potential of −80 mV. The records are corrected for linear leakage and capacitative currents. Bath solution contained 60 mM KCl + 60 mM NaCl. Horizontal and vertical calibrations are 100 ms and 1 μA, respectively.

mV, $n = 7$) dimer channels. A notable difference between D378T dimer (Fig. 3 *B*) and WT dimer (Fig. 3 *C*), however, can be seen in the marked reduction in the amplitude of inward tail currents (at 60 mM external $[K^+]$) elicited by the return step to −80 mV in the mutant channels. As discussed below, the basis of this effect is a marked change in the rectification characteristics of D378T channels.

Effects of D378T mutation on K conductance and selectivity

The current-voltage (I-V) relationship for fully activated WT $K_v2.1$ channels is known to display a Goldman-type rectification that depends on an asymmetric distribution of $[K^+]$ across the membrane (Frech et al., 1989). As shown in Fig. 4, *A* and *B*, the instantaneous I-V curve for the WT dimer channels (hereafter referred to as WT channels) obtained under symmetric $[K^+]$ conditions shows little curvature, suggestive of a symmetric energy profile for ion conduction in the pore (Jack et al., 1975). This profile is markedly disturbed, however, by the partial neutralization of negative charge associated with position 378 (hereafter referred to as D378T), such that the instantaneous I-V in symmetric $[K^+]$ showed an extreme outward rectification (Fig. 4, *C* and *D*).

A less obvious effect was a decrease in K/Na selectivity. As shown in Fig. 5, for WT channels (Fig. 5 *A*) recorded in a bathing solution containing 119 mM NaCl + 1 mM KCl we were unable to resolve inward tail currents. The apparent reversal potential (i.e., the potential at which outward current disappeared (Fig. 5 *C*, *open squares*)) was −88.0 ± 3.1 mV

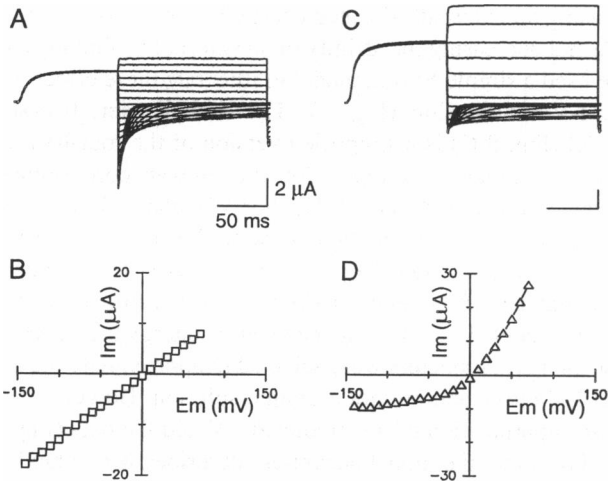

FIGURE 4 Instantaneous I-V relationships in WT $K_v2.1$ tandem dimers (*A* and *B*) and D378T mutant dimers (*C* and *D*). Whole cell tail currents were measured in isotonic KCl (120 mM KCl) solutions, using a two-pulse protocol in which channels were fully activated by conditioning pulses to +40 mV followed by test pulses to varying potentials (−140 to +70 mV). I-V relationships (*B* and *D*) for fully activated channels were obtained by plotting tail current amplitude, extrapolated to the beginning of the test pulse versus test pulse potential. The D378T mutation markedly suppressed slope conductance for inward currents (*D, lower left quadrant*) compared with outward currents (*D, upper right quadrant*). Vertical and horizontal calibrations are 2 μA and 50 ms, respectively.

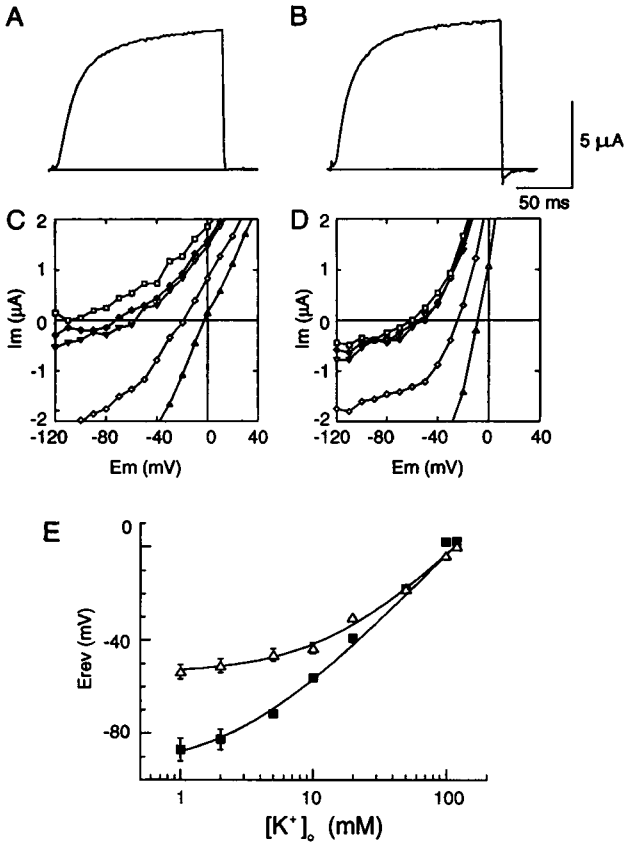

FIGURE 5 Effect of varying $[K^+]_o$ on the instantaneous I-V relationship in WT and D378T channels. Records shown in *A* and *B* are typical current traces obtained in bathing solutions containing 119 mM NaCl + 1 mM KCl. Currents were evoked by test pulse potential of +40 mV from a holding potential of −80 mV. Upon stepping to a return potential of −100 mV inward currents were observed in the D378T (*B*) but not in WT channels (*A*). *C* and *D* show whole cell I-V relationships obtained from peak tail currents evoked by conditioning potentials to +40 mV, from holding potential −80 mV, with return potential varying from −120 to +40 mV. The data are plotted with expanded ordinate scaling to emphasize shifts in reversal potentials. K^+ concentrations (mM) of 1 (□), 5 (◆), 10 (▽), 50 (◇) and 100 (△) were obtained in single oocytes that expressed either WT (*C*) or D378T (*D*) channels. *E* shows the relationship between reversal potential (E_{rev}) and $[K^+]_o$ in WT (■) and D378T (△) channels, from pooled data ($n = 4$ oocytes in both WT and D378T experiments). The smooth curves were fit to the data according to a modified Goldman relationship described in the text.

($n = 5$). In contrast, for D378T channels (Fig. 5 *B*) inward currents could be with reversal potential (Fig. 5 *D*, *open squares*) of −53.5 ± 3.0 mV ($n = 10$). The significantly more positive reversal potential suggests enhanced Na permeability. The point was explored further by determining the effect of varying $[K^+]_o$ and $[Na^+]_o$, in a reciprocal manner, on reversal potential (E_{rev}). Under these conditions inward currents can be detected in both WT and D378T channels (Fig. 5, *C* and *D*) at all but the lowest $[K^+]_o$ and true reversal potentials measured in almost all cases (except at 1 mM $[K^+]_o$ in WT channels). In the experiment illustrated by Fig. 5 *D* the reversal potential of D378T currents did not drop below −70 mV at the lowest $[K^+]_o$, and reversal potentials at $[K^+]_o$ in the range 1–10 mM varied much less than those obtained from WT currents at the same $[K^+]_o$ range (Fig. 5 *C*). These

results suggest that D378T channels, unlike WT, are measurably permeable to Na^+ ions. As shown in Fig. 5 *E* the relationship between E_{rev} and $\log_{10}[K^+]_o$ was nearly linear in WT (consistent with a nearly perfect potassium electrode) but markedly nonlinear in D378T (imperfect K/Na selectivity). We fit the data to a modified Goldman equation (Hodgkin and Horowicz, 1959):

$$E_{rev} = 59 \log_{10} \{([K^+]_o + \alpha [Na^+]_o)/[K^+]_i\}, \quad (2)$$

where α is the apparent selectivity ratio, P_{Na}/P_K. The data from WT channels were accurately fit by $\alpha = 0.02$ and $[K^+]_i = 143$ mM, whereas D378T data were fit by $\alpha = 0.10$ and $[K^+]_i = 140$ mM. Thus, the curvature in the plot indicates a fivefold reduction in the ability of the channel to discriminate between Na and K ions.

As indicated by reversal potential measurements (Table 1) the D378T mutation also impaired the ability of channels to discriminate between K and other, nonphysiological, metal cations. The deficiency, however, was not great enough to change the selectivity sequence: $P_K \gg P_{Cs} \gg P_{Na}$, which was the same in both WT and D378T channels.

Effects on K^+ conduction in the pore

The effect of D378T mutation on K conductance was explored in more detail by patch clamp measurement. As indicated in the whole cell data of Fig. 4 *D*, the limiting slope conductance of the outward limb of the I-V plot is nearly sevenfold greater than that of the inward limb. Under similar conditions the single channel conductance of WT is about 14 pS (Kirsch et al., 1992b). Thus, if we assume as a limiting case that the outward limb of the D378T mutant is unaffected and no changes in the probability of opening occurred, the inward limb of the mutant I-V curve would have a single channel conductance below the limit of resolution (i.e., <2 pS). This interpretation was confirmed by patch clamp measurements shown in Fig. 6. Inside-out patches in symmetric 120 mM KCl were pulsed to +80 mV to activate single channels and upon return to −80 mV in WT channels large inward currents were readily discerned in WT (Fig. 6 *A*), but not in D378T (Fig. 6 *B*) channels. Comparison of the single channel records shows that the mutation also affected outward currents. Their amplitude was reduced, although not nearly as much as the decrease in inward current amplitude, and the open time duration was reduced. Because of the latter effect, we were unable to quantify the amplitude of single channel currents in the outward direction by conventional interval analysis at the 0.5 kHz bandwidth required to distinguish open and closed levels. Instead, we used nonstationary fluctuation analysis (Sigworth, 1980) of macropatch currents at 10 kHz bandwidth. As shown in Fig. 7, at a test potential of +40 mV the estimated single channel current for D378T was 0.4 pA, compared with an average value of 0.6 pA in WT (obtained either directly from interval analysis, or indirectly from fluctuation analysis).

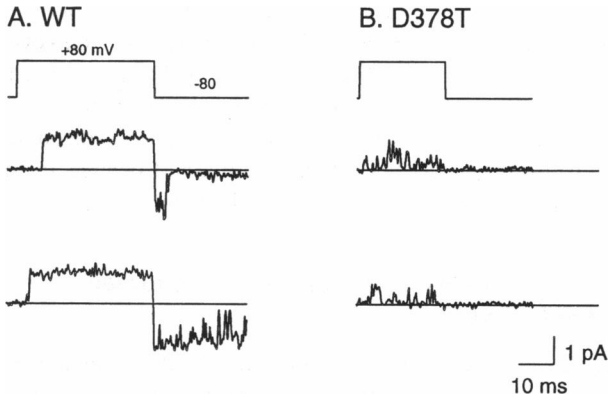

FIGURE 6 Single channel currents in cell-attached patches under approximately symmetric 120 KCl conditions. Oocytes were bathed in a depolarizing 120 mM KCl bath solution, and the patch pipette solution also contained 120 mM KCl. Representative traces were obtained from oocytes expressing either WT (*A*) or D378T (*B*) channels. For purposes of illustration the data were low pass filtered at 1 kHz.

Thus, the partial neutralization of negative charge contributed by Asp^{378} reduced inward K conduction through the pore to a much greater extent than outward conduction. These results can be explained if the aspartates at position 378 form a ring of negative charge at the external mouth of the pore. Partial neutralization would have the effect of increasing an externally-located energy barrier to ion conduction and decreasing the affinity of an external K binding site. We used a simple Eyring model to illustrate these effects on the I-V relationship (Fig. 8). The three-barrier, two-site model (Fig. 8 *C*) is a simplified version of the four-barrier, three-site model developed for the *Shaker* pore (Pérez-Cornejo and Begenisich, 1994). For WT channels we used voltage ramps to obtain single channel I-V curves over the range −80 to +100 mV (Fig. 8 *A*). As in *Shaker*, the I-V curve in symmetric $[K^+]$ shows a slight inward rectification that can be modeled by lowering the external energy barrier G34. The energy parameters were selected to approximate the actual I-V curve and are not a unique solution. However, the close superposition of the predicted I-V and the data (Fig. 8 *A*) shows that the model accurately describes K conduction through the WT pore under symmetric $[K^+]$ conditions. As shown in Fig. 8 *B–D*, by increasing the height of the external

TABLE 1 Ion selectivity in WT and D378T mutant channels, expressed in permeability ratio, P_X/P_K (n)

Channels	Rb	NH_4	Cs	Na
WT	0.83 ± 0.03 (5)	0.12 ± 0.01 (8)	0.11 ± 0.01 (5)	0.02 ± 0.01 (5)
D378T	0.97 ± 0.04 (5)	0.23 ± 0.03 (5)	0.30 ± 0.03 (6)	0.10 ± 0.01 (6)

P_X/P_K was determined from E_{rev} measurements in which 120 mM $[K^+]_o$ was replaced with the indicated cations, according to the formula (Hille, 1971): Log $(P_X/P_K) = (E_X - E_K)/58.5$, where E_X and E_K are reversal potentials obtained with ion, X, and K, respectively.

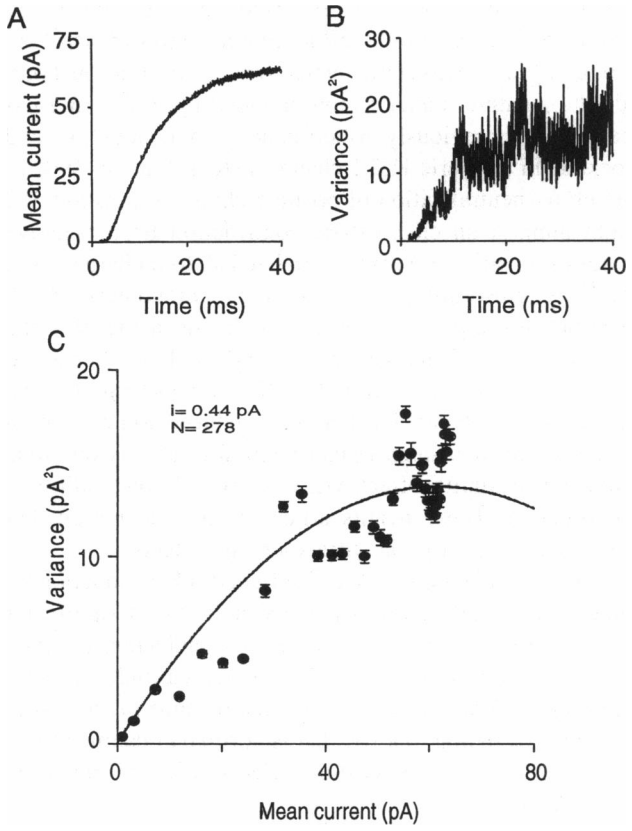

FIGURE 7 Nonstationary variance analysis of macropatch currents from D378T channels. Currents were recorded in cell-attached patches from oocytes bathed in a 120 mM KCl depolarizing solution. Patch pipette contained 120 mM KCl solution. *A* shows the time course of mean current evoked by a test potential of 40 mV from a holding potential of −80 mV. The ensemble average was obtained from 32 traces. *B* shows the time course of the variance, and *C* plots the variance as a function of the mean current. The parabolic curve is a best fit to the relationship between the variance and mean current described in the text, with $n = 278$ channels and $i = 0.44$ pA.

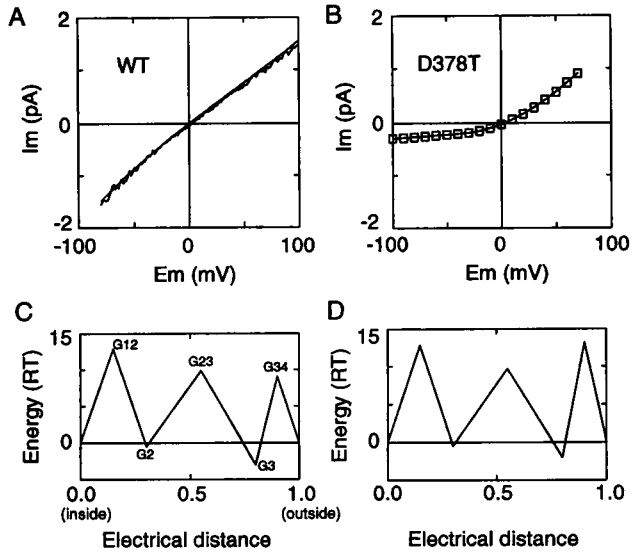

FIGURE 8 Rate theory model for K conduction in WT and D378T channels. *A* shows a typical single channel I-V curve in WT channels obtained by applying a ramp potential (−80 to +100 mV) to an inside-out patch bathed in isotonic (120 mM) KCl solution on both sides of the membrane. Sixteen traces were averaged after discarding closed intervals, to give the mean open channel I-V relationship. The superimposed, smooth curve shows the fit obtained from a two-barrier, three-well, rate theory model (*C*). For D378T (*B*), the single channel I-V curve was estimated from whole cell tail current amplitudes (Fig. 4 *D*) scaled according to the single channel current obtained by fluctuation analysis (Fig. 6 *C*) at +40 mV. The smooth curve shows the fit obtained from a rate theory model (*D*). *C* and *D*, respectively, show the energy profiles for K^+ ions as a function of electrical distance in the pore. The positions of the wells and barriers are approximately the same as those used previously to describe *Shaker* pores (Pérez-Cornejo and Begenisich, 1994). The maxima and minima were chosen to fit the $K_v2.1$ WT I-V curve. To fit the D378T I-V curve the energy profile was altered by increasing G3 from −3.0 to −2.0 RT and G34 from 9.1 to 13.2 RT where R and T have their usual thermodynamic meaning.

barrier G34 and reducing the depth of the external well, G3, we could reproduce the I-V relationship in the D378T mutant. These effects would be consistent with either a partial disruption of an ion interaction site within the outer part of the pore or by a localized reduction in K^+ concentration associated with the removal of negative surface charge in the external mouth. Either mechanism would result in reduced K^+ ion occupancy of the pore.

Effect of reduced ionic strength

In *Shaker* channels two conserved Gly residues, which in $K_v2.1$ correspond to Gly^{375} and Gly^{377} (Fig. 1), are critical for Na/K selectivity (Heginbotham et al., 1994). Given its close proximity and its effect on P_{Na}/P_K (Fig. 4 *E*), we would expect Asp^{378} to be part of the tunnel region closely associated with the selectivity filter, and therefore its effects on ion conduction should be those of a K-selective ion binding site. Its influence on ion conduction should be quite different from residues that lie just outside the tunnel, in which case long-range electrostatic effects should predominate. Charges in the wide mouth would be expected to influence ion conduction via through-space electrostatic interactions that increase local concentration of K^+ ions above that in bulk solution, whereas charged groups in the narrow, K-selective region should directly influence ion binding. Given that the former effect is strongly reduced by screening in a high ionic strength environment or by divalent ion binding, whereas the latter effect is primarily related to K concentration, it should be possible to distinguish tunnel and mouth residues by varying ionic strength at constant $[K^+]$. Thus, if Asp^{378} influences K conductance by localized K accumulation via through-space electrostatic attraction we would expect reduced ionic strength to potentiate the accumulation in WT channels, and to partially relieve the apparent depletion observed in D378T channels. However, as shown in Fig. 9, *A* and *B*, neither effect was observed. In the WT channels, contrary to expectation, when ionic strength, at a constant KCl (20 mM), was reduced by replacing LiCl with sucrose (Fig. 9 *A*, *inset*), currents were slightly reduced (*open triangle*). However, as indicated by the nearly unchanged I-V curve (Fig. 9 *A*), the effect was quite small. As shown in Fig. 9 *B*, neutralization of Asp^{378} markedly exaggerated the anomalous effects of

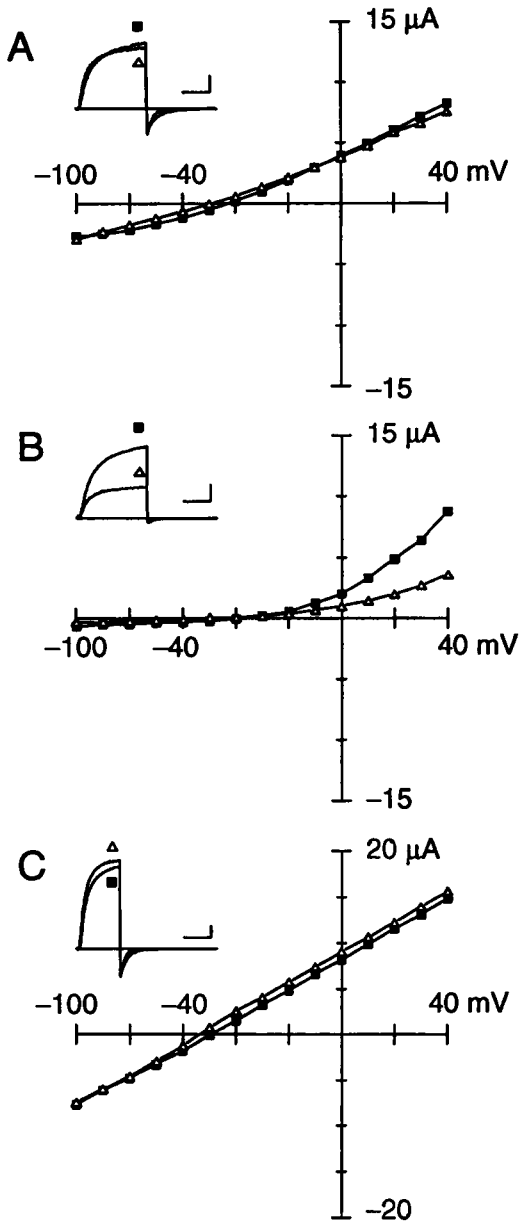

FIGURE 9 Effect of reduced ionic strength at constant 20 mM KCl on I-V relationships in WT (*A*), D378T (*B*), and K382C (*C*) channels. Normal ionic strength solution (125 mM, ■) contained (in mM): 20 KCl, 100 LiCl, 5 HEPES (pH 7.2 with Tris-OH). Reduced ionic strength solution (30 mM, △) was made by replacement of LiCl with 200 mM sucrose. The inset current traces were evoked by test potential, +40 mV; holding potential, −80 mV; and return potential, −100 mV. The vertical and horizontal calibrations are 2 μA and 50 ms, respectively.

ionic strength. Outward currents in D378T dimer channels (Fig. 9 *B*, *inset*) at a test potential of 40 mV were substantially reduced when the ionic strength was depleted (*open triangle*). Similar effects were observed on the inward limb of the I-V curve (not shown). These results argue that, in the mutant channels, the predominant electrostatic effect at reduced ionic strength is enhanced depletion caused by a nearby positive surface charge, rather than enhanced accumulation due to residual negative surface charge at position 378. Lys^{382} (Fig. 1) is a likely candidate for a positively charged residue that might influence ion binding at Asp^{378} by through-space electrostatic interactions, since it lies just outside the putative tunnel region bounded by Pro^{381}, and has been shown previously to influence ion conduction and blockade in chimeric $K_v2.1$ channels (Kirsch et al., 1992a). Therefore, neutralization of positive charge at position 382 might unmask an electrostatic contribution from negative charges at position 378. We neutralized all four charges from Lys^{382} by substituting Lys → Cys in a monomeric $K_v2.1$ construct, leaving Asp^{378} intact. As shown in Fig. 9 *C* the instantaneous I-V relationship at 20 mM $[K^+]_o$ was linearized by this mutation compared with WT channels (Fig. 9 *A* and Kirsch et al., 1992a). Furthermore, reduced ionic strength (Fig. 9 *C*, *open triangles*) had negligible effects on slope conductance (similar effects were observed in four additional experiments). These results argue against the notion that Asp^{378} acts primarily via surface-charge effects.

If the neutralization of Asp^{378} influences K conduction by reducing ion binding affinity, we would expect significant decrease in the ability of potassium-like molecules to block the pore. A variety of externally applied cationic blockers including TEA are known to enter and occlude the pore presumably by binding to a site that is normally occupied by K ions. Therefore, we assessed the effects of D378T mutation on blockade.

TEA block

TEA normally blocks WT $K_v2.1$ channels with relatively low affinity (IC_{50} = 5.5 mM) when applied externally, but higher affinity (0.2 mM) when applied internally (Taglialatela et al., 1991). Because of the negligible voltage dependence of block, the external TEA site probably lies just outside the membrane electric field. At least part of the site has been localized to the aromatic rings contributed by Tyr^{380} (Heginbotham and MacKinnon, 1992), such that TEA binding is potentiated by interaction with π-electrons of the four phenolic side chains. As shown in Fig. 10 *A*, in WT channels 5 mM TEA causes a substantial blockade which is rapid in onset and readily reversible. However, in D378T channels (Fig. 9 *B*), despite the presence of Tyr residues at position 380, partial neutralization of the Asp ring at 378 profoundly inhibited blockade. TEA at 5 and 50 mM blocked currents by <5%. Complete replacement of external monovalent ions with TEA-Cl (120 mM) resulted in a partial block that developed slowly and was almost irreversible upon washout. This block is almost certainly caused by the slow accumulation of TEA in the oocyte cytoplasm where it can bind to the high-affinity internal site, because it could not be washed out easily. Similar effects, due to the limited membrane permeability of quaternary ammonium ions applied to oocytes, were obtained previously at lower drug concentrations for the more lipophilic tetrapentylammonium ion (Taglialatela et al., 1991). Assuming that only the reversible component represents binding at the external site, we estimate that the IC_{50} in the mutant channels must be greater than 1 M, compared

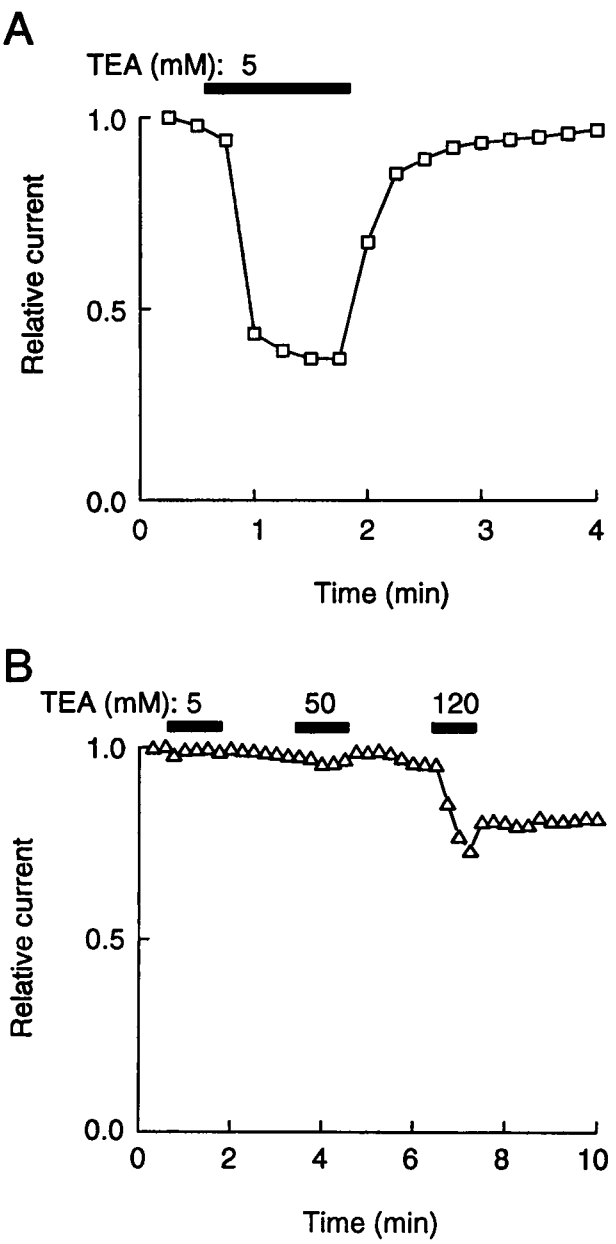

FIGURE 10 External TEA blockade in WT (*A*) and D378T (*B*) mutant channels. Test pulses to +40 mV were applied at 15-s intervals, and test pulse currents were normalized against control currents in the absence of drug. The horizontal bars above each graph indicate TEA application at the indicated concentrations (in mM). External bathing solution was 60 mM KCl + 60 mM NaCl.

with 3.0 ± 0.6 mM (n = 5) in the WT dimer channels. In contrast, we found that the sensitivity of D378T channels to internal TEA (applied by pressure injection through the voltage-recording pipette (Taglialatela et al., 1991); IC_{50}= 0.12 ± 0.03 mM, n = 6) was not significantly different from WT dimer channels (IC_{50}= 0.23 ± 0.07 mM, n = 5).

DISCUSSION

Asp^{378} is a conserved, negatively charged residue adjacent to the selectivity filter, which appears to form part of a major K ion binding site in the tunnel region of the pore. The conclusion that Asp^{378} is part of a binding site is based in part on the observation that K conductance and blockade by potassium analogs were adversely affected by the mutation. The same effects, however, might arise from neutralization of negative surface charge at peripheral, nonselective sites in the external mouth. The evidence against this interpretation is that decreased ionic strength of the external solution reduced the effectiveness of the remaining aspartates in the D378T dimer channel, rather than potentiating their effect on conductance, as would have been predicted from a through-space electrostatic mechanism. This anomalous behavior suggests the presence of nearby positive charge, which may be contributed by a nonconserved Lys residue at position 382. Indeed, neutralization of this residue enhanced conduction in the inward limb of the I-V curve but did not unmask a through-space electrostatic contribution when tested in reduced ionic strength conditions. Thus, the D378T mutation has effects quite distinct from carboxyl group neutralization by trimethyloxonium (TMO) applied to native K channels (MacKinnon and Miller, 1989b). In the latter case, TMO caused outward rectification in Ca-dependent K channels (K_{Ca}) only when measured under conditions of reduced ionic strength; no effect was observed at physiological salt concentrations. In our experiments, by contrast, strong rectification was observed even in isotonic KCl solution. This result together with the effects of D378T on Na/K selectivity argue in favor of locating Asp^{378} proximal to the tunnel region rather than at a distal site in the outer vestibule. In the TMO experiments of MacKinnon and Miller (1989b) the identity of the modified group or groups was unknown. The distinct difference from our results suggests that TMO was unable to modify the conserved Asp in K_{Ca} channels corresponding to Asp^{378}.

The effect of D378T on TEA block is particularly noteworthy because the D378T mutant channel contains tyrosines at position 380, the aromatic side chains of which have been identified previously as critical determinants of TEA block (Heginbotham and MacKinnon, 1992). The marked reduction in TEA block by replacement of two carboxylates with hydroxyl side chains in the D378T mutant shows that the external TEA site in K_v channels is formed not only by the phenolic rings of tyrosine (Tyr^{380}) side chains (Heginbotham and MacKinnon, 1992), but also by the carboxylate side chains of Asp^{378}. However, without performing more substitutions at position 378 we cannot rule out the possibility that the carboxylate influences TEA block indirectly by a through-space electrostatic effect, rather than as a direct participant in TEA binding. It should be noted, however, that in K_v2.1 the effect of replacing tyrosine at position 380 with cysteine in all four subunits (TEA IC_{50} = 35 mM) was much less than that of replacing aspartate at position 378 in only two of the four subunits (TEA IC_{50} > 1 M). A conservative view is that whereas Tyr^{380} is essential for conferring relatively high affinity TEA block to certain K_v isoforms, a necessary prerequisite to the formation of the binding site is the presence of negatively charged side chains

at position 378 as well. $K_v2.1$ WT contains both the prerequisite Asp and the high affinity-conferring Tyr380, yet its TEA sensitivity is ~10-fold less than that of $K_v3.1$, which contains the same critical residues. The difference is due to the presence of a positively charged Lys^{382} in $K_v2.1$, which is replaced by a neutral Gln residue in $K_v3.1$ (Kirsch et al., 1992a).

The notion that Asp^{378} is part of a K-selective site derives support from our observation that the P_{Na}/P_K selectivity ratio was significantly altered by mutation and by previous mutational results (Heginbotham et al., 1994) that identified Gly^{377} as a critical part of the Na/K selectivity filter. Unlike Gly^{377} mutations in monomeric *Shaker* constructs, however, D378T mutations in the $K_v2.1$ dimer did not convert the channel from a K-selective to a nonselective cation channel, since the selectivity sequence among widely different metal cations was preserved. At present we cannot distinguish between the possibilities that Asp^{378} is less critical than Gly^{377}, or that mutations of critical positions in the dimer are less disruptive than in the monomer. Our preliminary observations suggest that Gly^{377} mutations in the dimer construct also produce much less severe changes in selectivity than those reported by Heginbotham et al. (1994).

The P-regions of two other distantly related K channels, the *eag* channel (expressed from the *Drosophila ether à go-go* gene (Warmke et al., 1991)) and IRK1 (an inward rectifier cloned from mouse macrophage, Kubo et al., 1993) are naturally occurring variants in which Asn and Phe, respectively in *eag* and IRK1, replace the Asp, which is conserved in all K_v channels. The permeability of the *eag* channel to Na^+ relative to K^+, like that of our D378T mutant, is about 0.1 (Brüggemann et al., 1993). Although similar experiments have not been reported for IRK1 it would be interesting to perform reciprocal mutations of Asn, Phe, and Asp in the three sets of channels to sort out the significance of this position for specifying Na/K selectivity.

Our results are compatible with previous observations in cyclic nucleotide-gated (CNG) channels, which showed that neutralization of a negatively charged Glu in the P-region drastically reduced block by external cations (particularly divalent ions) and enhanced outward rectification (Root and MacKinnon, 1993; Eismann et al., 1994). This functional correspondence and the previous observation that neutralization of Asp in a GY-deleted *Shaker* channel eliminated block by external divalent cations (Heginbotham et al., 1992), supports the contention that these residues occupy homologous positions in the distantly related channels. A comparison of our results in K_v channels with those obtained in CNG channels suggests two major differences in the architecture of the channels. First, in CNG channels the voltage dependence of mutation-sensitive divalent block indicates a binding site located 35% of the distance through the membrane electric field, whereas in K_v channels the mutation-sensitive TEA site is much closer to the outer margin of the field. These results are consistent with the deeper location in the pore of Glu in CNG channels than Asp in K_v channels. Second, although Glu neutralization in CNG channels had no effect on permeability ratios, Asp neutralization in K_v channels significantly altered selectivity. However, it is not surprising that the residues play different roles in selectivity in view of the fact that, compared with K_v channels, WT CNG channels are quite nonselective and lack the GY doublet that is critical to ion selectivity in K_v channels (Heginbotham et al. 1992). We conclude therefore, that in K_v channels Asp^{378} has evolved from providing a relatively nonselective ion binding site to forming part of a K-selective ion binding site associated with the Na/K selectivity filter at the external mouth of the pore.

We thank W-Q. Dong and C-D. Zuo for expert oocyte injection and culture. We also thank Dr. L. Parent for comments on the manuscript, Dr. J. A. Drewe for help during the early stages of dimer construction, Dr. M. Taglialatela for single channel tests of the dimer stoichiometry, and Dr. A.M. Brown for his support and encouragement throughout the course of this project.

Our work was supported by National Institutes of Health grants NS29473 (G.E.K.) NS23877 and HI37044 (A.M.B.).

REFERENCES

Brüggemann, A., L. A. Pardo, W. Stühmer, and O. Pongs. 1993. *Ether-à-go-go* encodes a voltage-gated channel permeable to K^+ and Ca^{2+} and modulated by cAMP. *Nature.* 365:445–448.

Butler, A., S. Tsunoda, D. P. McCobb, A. Wei, and L. Salkoff. 1993. *mSlo*, a complex mouse encoding "Maxi" calcium activated potassium channels. *Science.* 261:221–224.

Drewe, J. A., H. A. Hartmann, and G. E. Kirsch. 1994. Potassium channels in mammalian brain: A molecular approach. In Ion channels of excitable cells. Methods in Neuroscience, Vol. 19. T. Narahashi, editor. Academic Press, San Diego. 243–260.

Eismann, E., F. Müller, S. H. Heinemann, and U. B. Kaupp. 1994. A single negative charge within the pore region of a cGMP-gated channel controls rectification, Ca^{2+} blockage, and ionic selectivity. *Proc. Nat. Acad. Sci. USA.* 91:1109–1113.

Frech, G. C., A. M. J. VanDongen, G. Schuster, A. M. Brown, and R. H. Joho. 1989. A novel potassium channel with delayed rectifier properties isolated from rat brain by expression cloning. *Nature.* 340:642–645.

Goldstein, S. A. N., D. J. Pheasant, and C. Miller. 1994. The charybdotoxin receptor of a *Shaker* K^+ channel: peptide and channel residues mediating molecular recognition. *Neuron.* 12:1377–1388.

Hartmann, H. A., G. E. Kirsch, J. A. Drewe, M. Taglialatela, R. H. Joho, and A. M. Brown. 1991. Exchange of conduction pathways between two related K^+ channels. *Science.* 251:942–944.

Heginbotham, L., T. Abramson, and R. MacKinnon. 1992. A functional connection between the pores of distantly related ion channels as revealed by mutant K^+ channels. *Science.* 258:1152–1155.

Heginbotham, L., Z. Lu, T. Abramson, and R. MacKinnon. 1994. Mutations in the K^+ channel signature sequence. *Biophys. J.* 66:1061–1067.

Heginbotham, L., and R. MacKinnon. 1992. The aromatic binding site for tetraethylammonium ion on potassium channels. *Neuron.* 8:483–491.

Heinemann, S. H., F. Conti, and W. Stühmer. 1992. Recording of gating currents from *Xenopus* oocytes and gating noise analysis. *Methods Enzymol.* 207:353–368.

Hille, B. 1971. The permeability of the sodium channel to organic cations in myelinated nerve. *J. Gen. Physiol.* 58:599–619.

Hodgkin, A. L., and P. Horowicz. 1959. The influence of potassium and chloride ions on the membrane potential of single muscle fibres. *J. Physiol.* 148:127–160.

Imoto, K., C. Busch, B. Sakmann, M. Mishina, T. Konno, J. Nakai, H. Bujo, Y. Mori, K. Fukada, and S. Numa. 1988. Rings of negatively charged amino acids determine the acetylcholine receptor channel conductance. *Nature.* 335:645

Jack, J. J. B., D. Noble, and R. W. Tsien. 1975. Nonlinear properties of

excitable membranes. *In* Electric current flow in excitable cells. Clarendon Press, Oxford. 224–260.

Kirsch, G. E., J. A. Drewe, H. A. Hartmann, M. Taglialatela, M. De Biasi, A. M. Brown, and R. H. Joho. 1992a. Differences between the deep pores of K^+ channels determined by an interacting pair of nonpolar amino acids. *Neuron.* 8:499–505.

Kirsch, G. E., J. A. Drewe, M. Taglialatela, R. H. Joho, M. De Biasi, H. A. Hartmann, and A. M. Brown. 1992b. A single nonpolar residue in the deep pore of related K^+ channels acts as a K^+:Rb^+ conductance switch. *Biophys. J.* 62:136–144.

Kubo, Y., T. J. Baldwin, Y. N. Jan, and L. Y. Jan. 1993. Primary structure and functional expression of a mouse inward rectifier potassium channel. *Nature.* 362:127–133.

MacKinnon, R., and C. Miller. 1989a. Mutant potassium channels with altered binding of charybdotoxin, a pore-blocking peptide inhibitor. *Science.* 245:1382–1385.

MacKinnon, R., and C. Miller. 1989b. Functional modification of a Ca^{2+}-activated K^+ channel by trimethyloxonium. *Biochem.* 28:8087–8092.

MacKinnon, R., and G. Yellen. 1990. Mutations affecting TEA blockade and ion permeation in voltage-activated K^+ channels. *Science.* 250:276–279.

Noda, M., H. Suzuki, S. Numa, and W. Stühmer. 1989. A single point mutation confers tetrodotoxin and saxitoxin insensitivity on the sodium channel II. *FEBS Lett.* 259:213–216.

Pérez-Cornejo, P., and T. Begenisich. 1994. The multi-ion nature of the pore in *Shaker* K^+ channels. *Biophys. J.* 66:1929–1938.

Root, M. J., and R. MacKinnon. 1993. Identification of an external divalent cation-binding site in the pore of a cGMP-activated channel. *Neuron.* 11:459–466.

Schreibmayer, W., H. A. Lester, and N. Dascal. 1994. Voltage clamping of *Xenopus laevis* oocytes utilizing agarose-cushion electrodes. *Pflügers Archiv.* 426:453–458.

Sigworth, F. J. 1980. The variance of sodium current fluctuations at the node of Ranvier. *J. Physiol.* 307:97–129.

Taglialatela, M., A. M. J. VanDongen, J. A. Drewe, R. H. Joho, A. M. Brown, and G. E. Kirsch. 1991. Patterns of internal and external tetraethylammonium block in four homologous K^+ channels. *Mol. Pharmacol.* 40:299–307.

Tang, S., G. Mikala, A. Bahinski, A. Yatani, G. Varadi, and A. Schwartz. 1993. Molecular localization of ion selectivity sites within the pore of a human L-type cardiac calcium channel. *J. Biol. Chem.* 268:13026–13029.

VanDongen, A. M. J., G. C. Frech, J. A. Drewe, R. H. Joho, and A. M. Brown. 1990. Alteration and restoration of K^+ channel function by deletions at the N- and C-termini. *Neuron.* 5:433–443.

Warmke, J., R. Drysdale, and B. Ganetzky. 1991. A distinct potassium channel polypeptide encoded by the *Drosophila eag* locus. *Science.* 252: 1560–1564.

Yang, J., P. T. Ellinor, W. A. Sather, J. -F. Zhang, and R. W. Tsien. 1993. Molecular determinants of Ca^{2+} selectivity and ion permeation in L-type Ca^{2+} channels. *Nature.* 366:158–161.